Available free online at www.medjchem.com

Mediterranean Journal of Chemistry

Mediterranean Journal of Chemistry **2024**, 14(1), 58-68

Theoretical Investigation of Aluminum Corrosion Inhibition Using Chalcone Derivatives

Thomas Aondof Nyijime [1,*], Habibat Faith Chahul [1], Panpe Iliya Kutshak [1], Abdullahi Muhammad Ayuba [2], Fater Iorhuna [2], Victor Okai [1], and Abdulrahman Hudu [3]

[1] Department of Chemistry, College of Physical Sciences, Joseph Sarwuan Tarka University, Makurdi, 970101, Nigeria

[2] Department of Pure and Industrial Chemistry, Faculty of Physical Sciences, Bayero University, Kano, 700241, Nigeria

[3] Department of Chemistry, Faculty of Natural and Applied Sciences, Nigerian Army University, Biu, 603108, Nigeria

Abstract: The corrosion of Aluminum is a critical issue in various industrial applications. Using computational methods, this study theoretically investigated the corrosion inhibition properties of two chalcone derivatives. The aim was to understand the molecular mechanisms underlying the inhibitory effect of chalcone derivatives on aluminum corrosion. Density functional theory calculations and molecular dynamics simulations were employed to predict the adsorption behavior and electronic properties associated with the interaction between chalcone derivatives and aluminum surfaces. The binding strength of the inhibitor molecules on aluminum surfaces is of the order HNP > HPP, which agrees with the experimentally determined inhibition efficiencies. Considering those mentioned above, our method will be helpful for rapid quantum chemical calculations and molecular dynamics simulation prediction of a potential inhibitor from many similar inhibitors and then for their logical synthesis for application in corrosion inhibition via a wet chemical synthetic route.

Keywords: Corrosion; Inhibition; Aluminum; Chalcone; Theoretical studies.

1. Introduction

Corrosion is a natural process involving the deterioration of materials, especially metals, due to their environmental reaction. Aluminum is a widely used metal with various applications due to its unique strength, flexibility, formability, workability, and good thermal and electrical conductivity. They find widespread application in the industrial sector, particularly in aviation, aerospace, automotive, military hardware, shipbuilding, batteries, and home appliances [1-5]. Their excellent mechanical and physical qualities make them desirable materials, including their weight-to-high strength ratio, strong machining properties, recyclability, current harvester, and corrosion resistance [2-5]. The development of a thin layer oxide coating is the source of aluminum resistance. But, this layer is not a strong enough barrier for reasonably long-term corrosion prevention. This is because Aluminum can react as an acid or a base, meaning that its oxide coating is soluble in alkaline and acidic environments but stable in neutral ones. The primary factors contributing to aluminum corrosion include exposure to moisture, oxygen, and aggressive environments such as acids, alkaline solutions, and water [6]. Corrosion of Aluminum can result in significant economic losses, particularly in industries where Aluminum is a critical component, such as aerospace, automotive, construction, and marine applications [7]. Effective corrosion inhibition strategies can help extend the lifespan of aluminum structures and reduce maintenance costs. Corrosion often necessitates the replacement of aluminum components, which contributes to environmental waste and increased energy consumption in manufacturing [8]. Implementing corrosion inhibitors can help promote sustainability by extending the service life of aluminum products. Chalcones are one of the most significant classes of flavonoids in the kingdom of plants [9]. They possess a large number of replaceable hydrogen atoms, which provides them with a broad range of biological activity

**Corresponding author: Thomas Aondof Nyijime*
Email address: thomasnyijime@gmail.com
DOI: http://dx.doi.org/10.13171/mjc02402281774nyijime

Received January 18, 2024
Accepted February 17, 2024
Published February 28, 2024

and derivatives, including antibacterial, anti-inflammatory, anti-cancer, anti-inflammatory, antimalarial, antiallergic, antioxidant, antiinfective, anti-influenza, and anti-protozoal properties [9–12]. However, they are still being used and shown to be effective as aluminum corrosion inhibitors in acidic environments. Chalcone derivatives have gained attention as potential corrosion inhibitors due to their favorable properties and ability to adsorb onto metal surfaces and form protective layers [13]. Chalcone derivatives are often considered environmentally friendly corrosion inhibitors. They are organic compounds that can be synthesized using the green chemistry principle, reducing the environmental impact of corrosion inhibition [14]. Fouda et al. [14] used four independent techniques (potentiodynamic polarization, electrochemical impedance spectroscopy (EIS), electrochemical frequency modulation (EFM), and weight loss measurements) to study the corrosion inhibition of Aluminum, in which the methods gave similar results. The aluminum metal corrosion was investigated in 0.5M HCl using some Chalcone derivatives as inhibitors. They found that the inhibitors were weakly adsorbed on the metal surface through a one-step process. Number of adsorption sites, charge density, molecular size, heat of hydrogenation, and formation of metallic complexes were the established factors controlling the corrosion inhibition of these chalcones. Chalcone derivatives typically exhibit low toxicity, making them suitable for various industrial applications where safety and environmental concerns are paramount [15]. Chalcone derivatives can also be combined with other corrosion inhibitors to achieve synergistic effects, enhancing their overall performance in corrosion protection [16]. Density Functional Theory (DFT) and Molecular Dynamics (MD) Simulations play crucial roles in predicting and understanding the behavior of corrosion inhibitors at the molecular level. This is so because it has been discovered that there are significant relationships between specific semi-empirical characteristics and the corrosion inhibition efficiency of most substances [17]. Recent research has examined the relationship between several corrosion inhibitors and metal surfaces using molecular dynamics simulations to compare many inhibitors' theoretical and practical effectiveness [18-24].

Determining which parameter has the most influence on raising the inhibitor efficiency might be challenging because factors related to the molecule's electrical and chemical structures frequently affect it simultaneously [24–27]. Because of this, the investigation's target substances were similar-structured organic compounds. The influence of the electrical structure is expected to be better studied, and the impact of the chemical structure is expected to be pretty similar. New organic corrosion inhibitors must continually be developed despite abundant organic molecules [28–30]. Studying the relationships between adsorption and corrosion inhibition is crucial because the adsorption of organic inhibitors on the surface of Aluminum can significantly alter its ability to resist corrosion [28]. Numerous factors, such as the kind and quantity of possible adsorption sites inside the inhibitor molecule, influence the adsorption properties of these inhibitors. There have been several attempts to correlate the efficacy of these compounds' corrosion inhibitors with several structural characteristics [3,4,14]. These compounds were selected based on molecular structural considerations; that is, they are organic substances with nearly identical chemical structures, and the primary reason for the variations in their inhibitory activities ought to be their disparate electronic structures. This study aims to investigate the corrosion inhibition of Aluminum by chalcone derivatives to provide an understanding of the underlying chemical and physical processes. The optimized chemical structures of the two chalcone derivatives namely 3-(4-hydroxyphenyl)-1-phenylprop-2-en-1-one (HPP) and 4-hydroxyphenyl)-1-(4-nitrophenyl) prop-2-en-1-one (HNP) are shown in Figure 1.

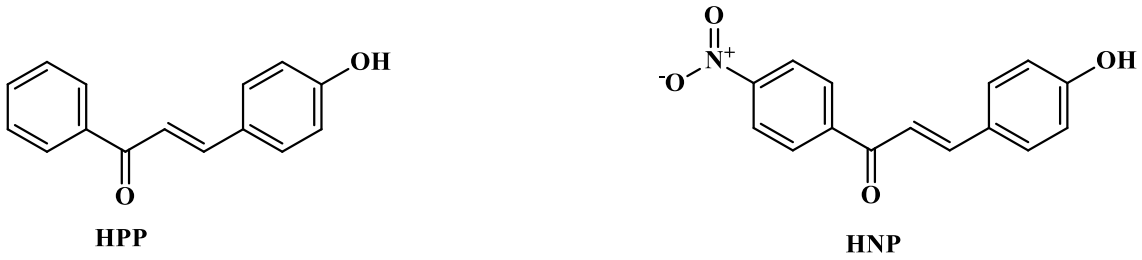

Figure 1. Optimized Chemical Structures of chalcone derivatives

2. Computational Details

Density functional theory (DFT) is a widely used computational method in quantum chemistry and solid-state physics for predicting the electronic structure and properties of molecules and materials. DFT is based on the concept that the total energy of a system is a function of the electron density. Chemdraw Ultra 7.0 was used to create sketches of the relevant inhibitor compounds. In order to improve the geometry of the molecules'

structures and reduce their torsional and conformational energy, geometry optimization was applied to all the molecules in the sketches. This was accomplished with the help of Accelrys Material Studio 7.0's DMol3 geometry optimization task. The improved structures were kept for future use in quantum calculations of some structural and electrical properties [17]. The electronic structure of the chalcone derivatives was evaluated to determine the active sites' local and global reactivities of the molecules. These included analyzing the distribution of frontier molecular orbitals, E_{HOMO}, $E_{LUMO,}$ and other quantum chemical parameters were studied investigate their corrosion inhibition performances. Local reactive site parameters of the chalcone derivatives have been analyzed through the Fukui indices. The chemical potential μ of a substance is expressed as [12,17-19].

$$\chi = -\mu = -\left(\frac{\partial E}{\partial N}\right)v(r) \quad (1)$$

According to Parr and Yang [19], the second derivative of E concerning N at a fixed v(r) is the definition of hardness (η) in the context of DFT.

$$\eta = \left(\frac{\partial E^2}{\partial N^2}\right)v(r) = \left(\frac{\partial u}{\partial N}\right)v(r) \quad (2)$$

$$I = -E_{HOMO} \quad (3)$$

$$A = -E_{LUMO} \quad (4)$$

$$\chi = \frac{IP+EA}{2} = -\frac{E_{LUMO}+E_{HOMO}}{2} \quad (5)$$

$$\eta = \frac{IP-EA}{2} = -\frac{E_{LUMO}-E_{HOMO}}{2} \quad (6)$$

$$\sigma = 1/\eta \quad (7)$$

$$\omega = \frac{\mu^2}{2\eta} = \frac{\chi^2}{2\eta} \quad (8)$$

$$\varepsilon = \frac{1}{\omega} \quad (9)$$

$$\Delta E_{b-d} = -\frac{\eta}{4} = \frac{1}{8}(E_{HOMO} - E_{LUMO}) \quad (10)$$

Using equation (11) and the predetermined values for x and η, the quantity of electrons that were transported from the inhibitor molecule to the surface of the Al metal was estimated.

$$\Delta N = \frac{(\chi Al - \boldsymbol{\chi inh})}{2(\eta Al + \eta inh)} \quad (11)$$

χ_{Al} and χ_{inh} stand for the absolute hardness of the aluminum metal and the inhibitor molecule, respectively, and η_{Al} and η_{inh} for the absolute electronegativity of the metal and inhibitor molecule, respectively. By assuming that for a metallic bulk, I = A, theoretical assumptions included the bulk aluminum electronegativity of χ_{Al}=5.6 eV and its global hardness η_{Al} = 0 [31]. The second-order Fukui function is a powerful tool for identifying and characterizing electrophilic and nucleophilic sites in molecules. The second-order Fukui function, often denoted as f^2, represents the electronic density change at a specific atomic site when one electron is added (f^+) or removed (f^-) from the system while keeping the total number of electrons constant.

F^+ (Nucleophilic Fukui Function): It describes the susceptibility of an atom to act as a nucleophile, indicating the tendency to donate electrons or participate in electron-rich reactions.

F^- (Electrophilic Fukui Function): It describes the susceptibility of an atom to act as a nucleophile, indicating the tendency to donate electrons or participate in electron-deficient reactions [32-33].

2.1. Molecular Dynamic Simulations

The Al(1 1 0) surface, the most stable atom-for-atom, was utilized to mimic every chemical complex. The FORCITE tools included in BIOVIA Material Studio 7.0 were used to run the simulation. In a simulation box measuring 17 by 12 by 28, computations were carried out using the COMPASS force field and Smart algorithm to model a representative surface region. At a fractional depth of 3.0 Å, the aluminum crystal was split along the (1 1 0) plane. The bottom layers' geometry was constrained before the surfaces were optimized and expanded into a 5 x 5 supercell to avoid edge effects by appropriately fitting the investigated molecule. By maintaining the temperature at 350K, a compromise was achieved between a system with excessive kinetic energy, in which the molecule desorbs from the surface, and a system with inadequate kinetic energy, in which the molecule cannot travel across the surface. With a simulation length of 5 ps and a time step of 1 fs, the temperature was set using the NVE (microcanonical) ensemble. The system was set up to quench every 250 steps, allowing for a maximum of 20 quench cycle combinations. FORCITE optimized the architectures of the molecules and surfaces to obtain the different interactions of the molecules with the surfaces. The Al (1 1 0) surface generated for the simulations was big enough to fit it and suitably tuned to avoid ghost molecule edge effects that might interfere with the calculations [32-37]. The adsorption energy between each inhibitor and the Al(1 1 0) surface was calculated using the relationship displayed in equation (16).

$$E_{Adsorption} = E_{total} - (E_{inhibitor} + E_{Al\ surface}) \quad (16)$$

Where EAdsorption denotes the energy of adsorption, Etotal denotes the combined energy of the molecule and the Al(1 1 0) surface, Einhibitor denotes the energy of the chemical complex alone, and EAl surface denotes the energy of the Al (1 1 0) surface alone.

The binding energy of the compound on the Al(1 1 0) surface is given by equation (17):

$$E_{binding} = -E_{Adsorption} \quad (17)$$

3. Results and Discussion

3.1. Molecular Dynamics Simulation

The adsorption behavior of two inhibitory compounds on aluminum metal (110) surfaces was investigated using molecular dynamics simulation incorporated in Material Studio. The top and side views of the molecules in their lowest energy forms on the Al(1 1 0) metal surface are shown in Figure 2. It could be observed that the molecule's benzenoid structure gives the molecules a flat-lying orientation on the metal surface and that most of their atoms have good surface interaction. The equilibrium configuration of the two inhibitors adsorbed on the Al (110) metal surface suggests that both chalcone compounds can adsorb on Al through the alkyl chain, phenyl ring, and heteroatoms, which are almost perpendicular to the surface. Table 1 presents the values of the two inhibitors' interaction and binding energies on the Al (110) metal surface. İt is evident that all the binding energies were positive. The larger the threshold value of binding energy, the easier the inhibitor adsorbs on the surface and the more effective. According to experiment findings, HNP has higher inhibitor efficiency since its binding energy is higher than that of HPP. This result is consistent with the experimentally determined value [9-12,14].

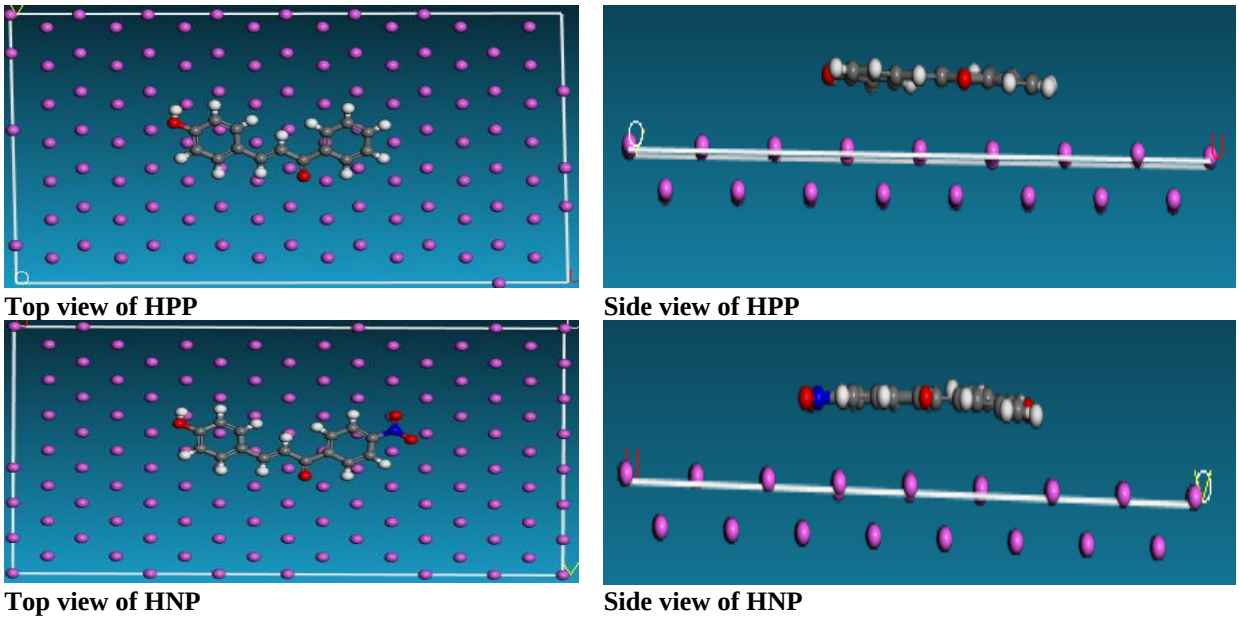

Figure 2. Al(1 1 0) Metal Surface configuration of adsorbed HPP and HNP molecules

Table 1. The two inhibitor's interaction and binding energy on the Al(110) metal surface.

Inhibitor	$E_{Al\text{-}inhibitor}$ (kJ/mol)	$E_{binding}$ (kJ/mol)
HPP	-87.953±0.0	55.473±0.0
HNP	-63.756±0.0	55.825±0.0

3.2 Equilibrium geometry structure

A molecule's lowest-energy configuration is called the "equilibrium geometry structure". The parameters for optimum bond length bond angle are shown in Table 2. To reduce the potential energy, atoms are spaced apart as much as possible. Bond lengths are usually at equilibrium when they are at the minimum of the potential energy curve for that specific bond. Additionally, angles between joined atoms are tuned to match the lowest possible energy state. It is evident from Table 2 that the bond length of C_3-O_4 in the HPP ring is 2.807 nm, longer than the common C-C single bond in (C_1-C_2, C_5-C_6, C_7-C_8, C_9-C_{10}, C_{11}-C_{12}, C_{13}-C_{14}, C_{15}-C_{16}) with variable comparable bond distance, and O_4-C_5 is 2.384 nm, longer than all of the C-C double in (C_2-C_3, C_6-C_7, C_8-C_9, C_{12}-C_{13}, C_{14}-C_{15}) which also have a comparable bond distance. The average bond distance indicates the conjugation has occurred at the hydroxyl unit of the phenyl ring. This conjugation action results in the development of a rigid planar structure in the corresponding HPP ring, which restricts the rotation of C-O in the phenyl rings following this restriction. Since one of the benzene rings in HPP (Figure 1) is joined to a hydroxyl group, it may be concluded that the lengths of all the C-C bonds fall between 1.348 and 1.456, providing ample evidence of the conjugation effect.

Table 2 clearly shows that the range of 1.355–1.464, smaller than the distance between C–O bonds, encompasses all C–C single and double bonds. Average bonds' tendency to form longer indicates conjugation of the HNP ring. Table 2 illustrates that the total bond angles of HNP and HPP molecules are from 118.965 to 127.4570. These angles are closer together, up to 1200, which causes their atoms to be sp2 hybridized [26-28].

Table 2. Bond length (Å), and bond angle (°) of inhibitor molecules in their optimal neutral form.

Geometry parameters	HPP	HNP
Bond length		
C_1-C_2	1.456	1.464
C_2-C_3	1.348	1.355
C_3-O_4	2.808	2.820
O_4-C_5	2.384	2.378
C_5-C_6	1.400	1.402
C_6-C_7	1.388	1.386
C_7-C_8	1.398	1.395
C_8-C_9	1.397	1.393
C_9-C_{10}	1.395	1.393
C_{10}-C_{11}	5.326	-
C_{11}-C_{12}	1.401	-
C_{12}-C_{13}	1.394	-
C_{13}-C_{14}	1.399	-
C_{14}-C_{15}	1.388	1.404
C_{15}-C_{16}	1.381	1.390
C_{16}-C_{17}	3.623	1.399
C_{17}- O_{18}	-	1.388
C_{18}-C_{19}	-	1.380
Bond angle		
C_1-C_2-C_3	120.659	118.965
C_3-C_4-0_4	57.873	57.815
C_5-C_6-C_7	120.969	121.221
C_6-C_7-C_8	119.660	119.019
C_7-C_8-C_9	119.893	121.085
C_8-C_9-C_{10}	120.360	119.248
C_2-C_3-C_{11}	127.457	-
C_3-C_{11}-C_{12}	124.387	-

3.3 Frontier Orbital Energies

Given that elements about molecules' electrical and chemical structures sometimes affect them simultaneously, it may be difficult to pinpoint which parameter has the most significant impact on increasing the inhibitor efficiency. Figure 3 depicts the orbitals of the HOMO and LUMO of the two molecules. The hetero atoms nitrogen, oxygen, and hydroxyl are all present in the functional group of the Chalcone derivatives, and they all contribute significantly to the suppression of metal corrosion. The phenylprop functional group is where the HOMO orbitals are discovered to be located in HPP, whereas the hydroxyl and nitro groups were found in HPN. The benzene - bonds were the center of the LUMO orbitals of every molecule under study [9-12,14,26].

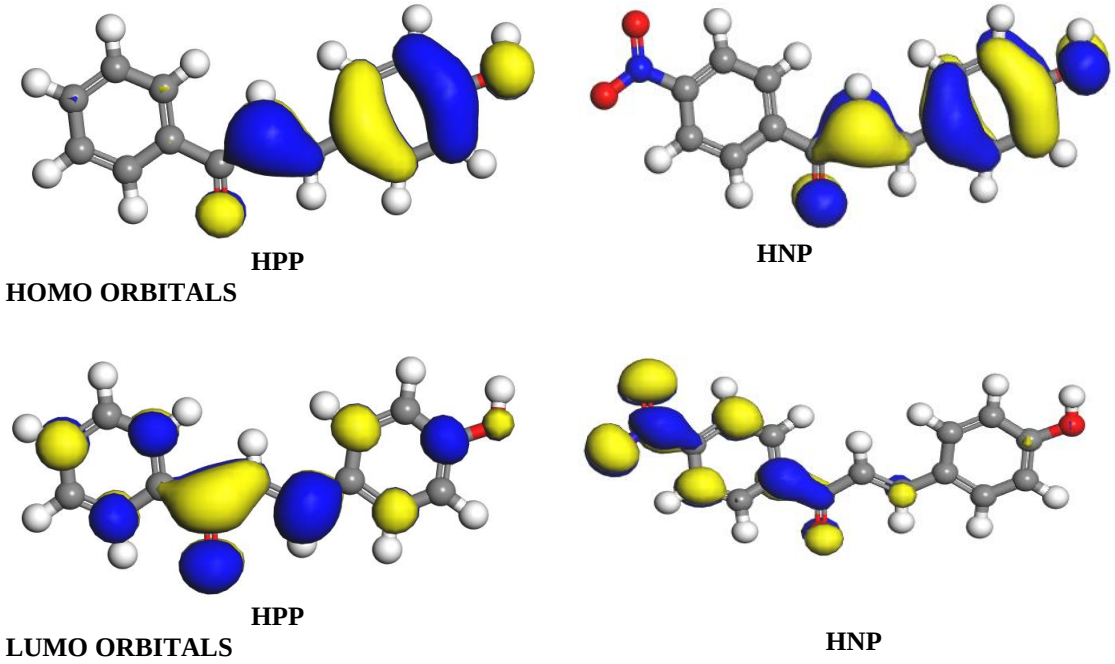

Figure 3. Orbitals of HOMO and LUMO of HPP and HNP molecules

The analysis of these molecules yields assessments of the following quantum chemical properties: electronegativity (χ), dipole moment (μ), energy gap (ΔE), global hardness, global softness, global electrophilicity index (ω), nucleophilicity (ε), energy of back donation (ΔEb-d), fraction of electron(s) (ΔN) transferred from the molecule to the metal (N), E_{HOMO} and E_{LUMO}. These quantum characteristics reveal the metal inhibition potentials of the inhibitor compounds [7,17]. The determined parameters are presented in Table 3. The highest-energy molecular orbital (E_{HOMO}), denotes the area of a molecule rich in electrons. Increasing values of E_{HOMO} indicate that the inhibitor molecules have a solid inclination to transfer electrons to the suitable acceptor molecule, which possesses an empty molecular orbital. The lowest-energy unoccupied molecular orbital (E_{LUMO}) is orbital to which electrons are most likely to be added during chemical reactions and indicates the electron-poor region of a molecule. Decreasing values of E_{LUMO} signify the probability that a molecule would accept an electron increases [38]. Relative energies of the HOMO and LUMO can be used to determine the reactivity of a molecule (energy gap). A small HOMO-LUMO gap can reveal a molecule's vulnerability to different reactions, including electrophilic or nucleophilic attack, and is frequently linked to greater chemical reactivity [8]. It can be inferred from the relative energies of its LUMO and HOMO that the inhibitory potential of the molecules is of the order: HNP> HPP [12,14]. Electronegativity measures an atom's relative propensity to draw shared electrons in a covalent link. The studied inhibitor molecules' electronegativity is of the order HNP> HPP. The polarity of a molecule is expressed as a dipole moment. In our study, the dipole moment follows the order HNP> HPP, demonstrating that HNP is more effective at donating electrons than HPP since it has the largest charge separation, the lowest stability, and the highest reactivity [39]. Ionization energy is needed to extract an electron from an atom or an ion. The ionization energy and electron affinity are correlated. The ionization energy and electron affinity of the present study are of the order HNP>HPP, which is in good agreement with the experimentally determined values. Global softness and hardness are utilized to shed light on the stability and reactivity of molecules.

Resistance to electron transport and stability are implied by high global hardness. Reactivity and a propensity for electron transport are implied by low global hardness. The values obtained for this study also agree with the experimentally determined values [9-14].

Table 3. Calculated quantum chemical parameters of the studied molecules.

Properties	HPP	HNP
E_{HOMO} (eV)	-6.019	-6.206
E_{LUMO} (eV)	-2.307	-3.687
ΔE (eV)	-3.712	-2.529
μ (Debye)	2.110	2.310
IE (eV)	6.019	6.206
AE V	2.307	3.687
χ (eV)	4.163	4.947
η (eV)	1.856	1.259
σ $(eV)^{-1}$	0.539	0.794
ω (eV)	4.669	9.719
ε $(eV)^{-1}$	0.214	0.103
ΔE_{b-d} (eV)	-0.464	-0.316
ΔN	0.387	0.259
CosAr(A^2)	259.14	289.65
CosVol(A^3)	261.14	292.83

A molecule's reactivity can be inferred from the global electrophilicity index (ω). It is more probable for a molecule to behave as a strong electrophile if its electrophilicity index is high [40]. A molecule with a low ω value is less likely to engage in nucleophilic assault processes [28]. The present study's global electrophilicity index (ω) follows the order: HNP>HPP. A chemical species, usually an ion or molecule, can give up two electrons and create a new covalent bond with an electrophilic (electron-deficient) species known as nucleophilicity (ε). High nucleophilicity species are highly reactive and willing to release electrons when reacting chemically. Low nucleophilicity species are less reactive and eager to contribute electrons to chemical processes. It is evident from Table 3 that HPP is more reactive than the HNP molecule. The energy of back donation (ΔE_b-d) is a parameter that characterizes the transfer of electron density from a metal center to a ligand. When the ΔE_b-d number is positive, energy is needed for back donation. When back donation occurs, energy is liberated, according to a negative ΔE_b-d value. As can be observed from Table 3, the energy of back donation is all negative, suggesting the molecules exhibit a covalent character [41-42]. The difference in electron density between the molecule and the metal center during the formation of a complex or reaction is measured by ΔN. Electrons are moved from the molecule to the metal when the ΔN is positive. When there is a negative ΔN, electrons move from the metal to the molecule. This implies that the metal center donates electron density back to the molecule, forming a coordination link where the metal donates electrons [43]. The obtained ΔN values for the studied molecules are all positive, suggesting that all the inhibitor molecules' electrons are transferred to the metal surface. This result is similar to Nyijime and Iorhuna's [31].

A molecule's effective volume during its interactions with a solvent is measured by its CosVol. Greater volume and length of contact between the solute molecule and the solvent are indicated by larger CosVol values. Small CosVol values suggest a more limited or compact interaction between the solute molecule and the solvent [44-45]. CosAr measures a molecule's effective surface area exposed to a solvent. It displays the region of interaction between the solvent and the solute.

Greater CosAr values imply a more extensive surface area of the solute molecule in contact with the solvent. Reduced CosAr values suggest that the solute molecule is interacting with the solvent through a reduced exposed surface area. With rising values of CosAr and CosVol, it was discovered that the inhibitors' efficiency in inhibiting growth increased [44]. The inhibition performances of chalcone derivatives were similar to those obtained by [9-14,26].

Table 4. Analysed Molecules Fukui indices.

		Nucleophilic attack (f^+)		**Electrophilic Attack (f^-)**	
Compound	Atom	Milliken	Hirshfield	Milliken	Hirshfield
HPP	O_4	0.146	0.133	0.073	0.066
HNP	O_{13}	0.208	0.191	0.166	0.160

3.4 Fukui Function

The tendency of an atom or molecular site to receive electrons grows with the system's electron density, and this tendency is represented by the nucleophilic Fukui function f^{+}. A high positive f^{+} value indicates a site that readily takes in electrons. The inclination of an atom or molecular site to donate electrons when the electrophilic Fukui function, f represents the electron density drops^{-}. An electron-donating site with a high positive f^{-} value has the potential to be nucleophilic, which means it can attack electrophiles [46-47]. It can be seen from Table 4 that the oxygen (O) atom acts in both molecules as either an electrophile or a nucleophilic attack. Since oxygen has the highest value among all other atoms in the molecule. The graphical representation of the second Fukui function and the computed values are presented and tabulated in Figure 4a-b and Table 5, respectively. A molecule's reaction to the addition or subtraction of two electrons is connected to the Second Fukui Function. When two electrons are added to a particular site, the electron density rises, as shown by positive f^2 values. This indicates that the location is electrophilic, meaning it tends to take electrons. The electron density at the location falls when two electrons are removed, according to negative f^2 values [48-49]. This suggests an electron-donating inclination, which makes the location nucleophilic. As can be observed from Table 5, 96.55% of the electrons in the HPP molecule are positive, while 3.55% are negative, which suggests the tendency of electrophilicity is higher than nucleophilicity. In the HNP molecule, 77.42% are positive, while 22.58% are negative. Fukui Function plots (Figures 4a–b) graphically display the Second Fukui Function f2. Negative values denote nucleophilic sites, whereas positive values suggest electrophilic sites. As shown in Figure 4a-b, the ratio of electrophilic site attacks is higher compared to nucleophilic site attacks [26].

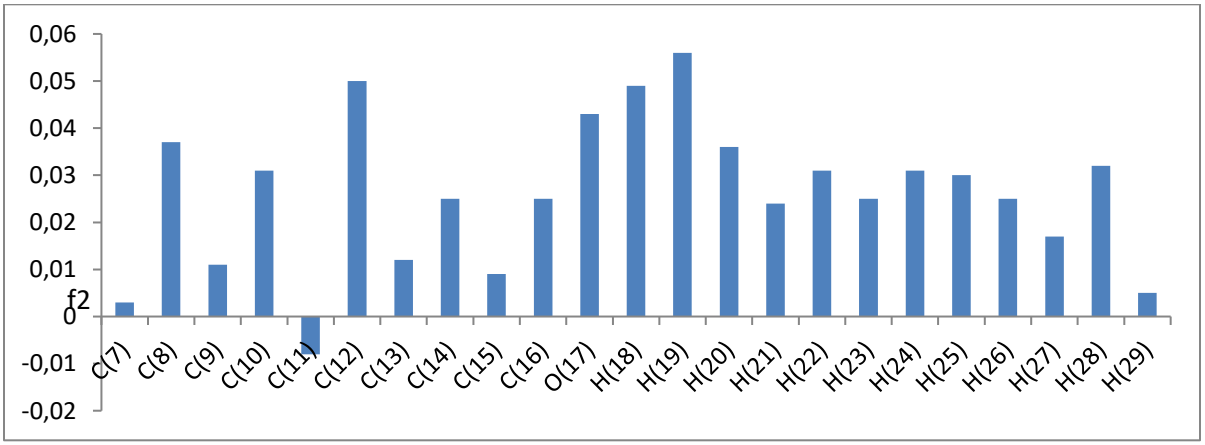

Figure 4a. Second Fukui Function plot for HPP molecule

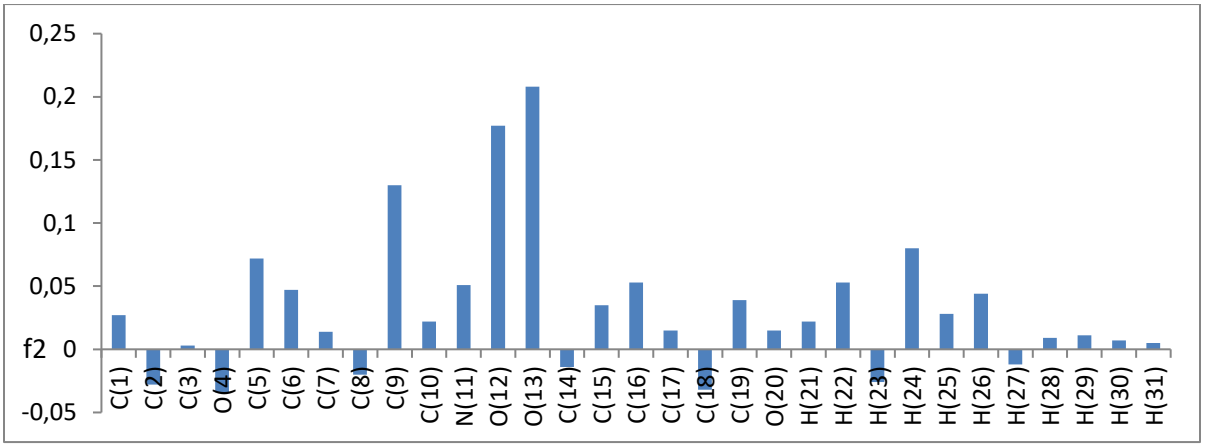

Figure 4b. Second Fukui Function plot for HNP molecule

Table 5. Second Fukui function percentage of the inhibitor Molecules.

Molecule	F^{2+}%	F^{2-}%
HPP	96.55	3.55
HNP	77.42	22.58

4. Conclusion

The structure and stability of the corrosive solutions and the interactions between Aluminum and the chalcone derivatives were examined using simulation and theoretical calculations. The outcomes demonstrate that using chalcone derivatives can greatly slow down aluminum corrosion. The primary mechanism responsible for inhibiting corrosion is the adsorption of chalcone derivatives onto the aluminum surface, which develops an adsorbate-substrate complex. Moreover, HNP was a more promising inhibitor than HPP on the aluminum surface due to its high adsorption and binding stability, which agrees with the experimentally determined value. This can result from variations in the heteroatom kinds and molecular sizes found in the various compounds. Considering the aforementioned, our method will be helpful for rapid quantum chemical calculations and molecular dynamics simulation prediction of a potential inhibitor from many similar inhibitors and for their logical synthesis for application in corrosion inhibition via a wet chemical synthetic route.

Acknowledgments

The authors thank Dr. Arthur Ebuka David, Department of Pure and Applied Chemistry, University of Maiduguri, Borno State, Nigeria, for the BIOVIA Materials Studio software.

References

1. A. Al-Hashem, M. Lowther, J. Al-Besharah, H.M. Shalaby, Industrial corrosion and corrosion control technology, Kuwait Institute for Scientific Research, **1996**, 449-500.
2. B. Valdez, M. Schorr, R. Zlatev, M. Carrillo, M. Stoytcheva, L. Alvarez, N. Rosas, Corrosion control in industry, Environmental and Industrial Corrosion-Practical and Theoretical Aspects, **2012**.
3. A. Celik-Kucuk, T. Abe, Lithium trifluorosulfonimide salt containing siloxane-based electrolytes for lithium-ion batteries: Aluminum corrosion behaviors and electrochemical properties, Journal of Power Sources, **2023**, 556, 232520.
4. C. L. Li, S.W. Zeng, W. Peng, Z.J. Li, Y. Li, D.N. Zhao, S.Y. Li, Mechanism of aluminum corrosion in LiFSI-based electrolyte at elevated temperatures, Transactions of Nonferrous Metals Society of China, **2021**, 31(5), 1439-1451.
5. A. Celik-Kucuk, T. Abe, Salt-Concentrated Siloxane-Based Electrolytes for Lithium Metal Batteries: Physical Properties, Electrochemical Properties, and Cell Performance, ACS Applied Energy Materials, **2023**, 6(9), 4618-4629.
6. M.A. Wahid, A.N. Siddiquee, Z.A. Khan, Aluminum alloys in marine construction: characteristics, application, and problems from a fabrication viewpoint, Marine Systems & Ocean Technology, **2020**, 15, 70-80.
7. J. Jung, S. Oh, H. Kwon, Effects of environmental factors on corrosion behaviour of aluminum, Materials and Corrosion, **2021**, 72(3), 557-563.
8. M.A.A. Khan, O.M. Irfan, F. Djavanroodi, M. Asad, Development of Sustainable Inhibitors for Corrosion Control, Sustainability, **2022**, 14(15), 9502.

9. W. Mecibah, H. Allal, M. Cherifi, S. Bouasla, B. Nabila, Theoretical study of chalcone derivatives as corrosion inhibitors for Aluminum in acidic environment, Rev. Roum. Chim., **2021**, 66(7), 633-644.
10. A.M. Maharramov, Y.V. Mamedova, M.R. Bayramov, I.G. Mamedov, Chalcone derivatives as corrosion inhibitors for mild steel in brine-kerosene solution, Russian Journal of Physical Chemistry A, **2018**, 92, 2154-2158.
11. S. Velrani, R. Mahalakshmi, Investigation of inhibition effect of naphthyl chalcones on mild steel corrosion in sulphuric acid medium, Rasayan J. Chem., **2015**, 8, 156-160.
12. A.S. Fouda, M. Abdallah, M. Eissa, Corrosion inhibition of Aluminum in 1 M phosphoric acid solutions using some Chalcones derivatives and synergistic action with halide ions, African Journal of Pure and Applied Chemistry, **2013**, *7*(12), 394-404.
13. A. Chaouiki, H. Lgaz, R. Salghi, M. Chafiq, H. Oudda, K.S. Bhat, I.M. Chung, Assessing the impact of electron-donating-substituted chalcones on inhibition of mild steel corrosion in HCl solution: Experimental results and molecular-level insights, Colloids and Surfaces A: Physicochemical and Engineering Aspects, **2020**, 588, 124366.
14. A.S. Fouda, A.M. Eldesoky, A.F. Hassan, A. Abdelhakim, Performance and Theoretical Study on Corrosion Inhibition of 304 SS in Hydrochloric Acid Solutions by Chalcone Compounds, International Journal, **2014**, 2(3), 280-300.
15. M.Hrimla, L. Bahsis, M.R. Laamari, M. Julve, S.E. Stiriba, An overview on the performance of 1, 2, 3-triazole derivatives as corrosion inhibitors for metal surfaces, International Journal of Molecular Sciences, **2021**, 23(1), 16.
16. H. Lgaz, K.S. Bhat, R. Salghi, S. Jodeh, M. Algarra, B. Hammouti, A. Essamri, Insights into corrosion inhibition behavior of three chalcone derivatives for mild steel in hydrochloric acid solution, Journal of Molecular Liquids, **2017**, 238, 71-83.
17. T.A. Nyijime, H.F. Chahul, A.M. AYuba, F. Iorhuna, Theoretical Investigations on Thiadiazole Derivatives as Corrosion Inhibitors on Mild Steel. Advanced Journal of Chemistry-Section A, **2023**, 6(2), 141-154.
18. S.K. Saha, M. Murmu, N.C. Murmu, I.B. Obot, P. Banerjee, Molecular level insights for the corrosion inhibition effectiveness of three amine derivatives on the carbon steel surface in the adverse medium: a combined density functional theory and molecular dynamics simulation study, Surfaces and interfaces, **2018**, 10, 65-73.
19. R.G. Parr, W. Yang, Density-functional theory of the electronic structure of molecules, Annual review of physical chemistry, **1995**, 46(1), 701-728.
20. K.F. Khaled, Studies of iron corrosion inhibition using chemical, electrochemical and computer simulation techniques, Electrochimica Acta, **2010**, 55(22), 6523-6532.
21. H. Lgaz, S. Masroor, M. Chafiq, M. Damej, A. Brahmia, R. Salghi, I.M. Chung, Evaluation of 2-mercaptobenzimidazole derivatives as corrosion inhibitors for mild steel in hydrochloric acid, Metals, **2020**, 10(3), 357.
22. S.K. Saha, A. Hens, N.C. Murmu, P. Banerjee, A comparative density functional theory and molecular dynamics simulation studies of the corrosion inhibitory action of two novel N-heterocyclic organic compounds along with a few others over steel surface, Journal of Molecular Liquids, **2016**, 215, 486-495.
23. A. Singh, K.R. Ansari, P. Banerjee, M. Murmu, M.A. Quraishi, Y. Lin, Corrosion inhibition behavior of piperidinium based ionic liquids on Q235 steel in hydrochloric acid solution: experimental, density functional theory and molecular dynamics study, Colloids and Surfaces A: Physicochemical and Engineering Aspects, **2021**, 623, 126708.
24. P. Udhayakalaa, T.V. Rajendiranb, S. Gunasekaran, Theoretical study using DFT calculations on inhibitory action of some pyrazole derivatives on steel, Journal of Advanced Scientific Research, **2013**, 4(02), 31-37.
25. K.F. Khaled, M.M. Al-Qahtani, The inhibitive effect of some tetrazole derivatives towards Al corrosion in acid solution: Chemical, electrochemical and theoretical studies, Materials Chemistry and Physics, **2009**, 113(1), 150-158.
26. A.M. Ayuba, T.A Nyijime, Theoretical study of 2-methyl benzoazole and its derivatives as corrosion inhibitors on aluminium metal surface, Journal of Applied Science and Environmental Studies, **2021**, 4(2), 4-2.
27. A. Popova, M. Christov, T. Deligeorgiev, Influence of the molecular structure on the inhibitor properties of benzimidazole derivatives on mild steel corrosion in 1 M hydrochloric acid, corrosion, **2003**.
28. E.E. Ebenso, P.C. Okafor, U.J. Ekpe, Studies on the inhibition of aluminum corrosion by 2-acetylphenothiazine in chloroacetic acids, Anti-Corrosion Methods & Materials, **2003**, 50, 414-421.
29. E. McCafferty, H. Leidheiser, Corrosion Control by Coating, Science Press, Princeton, **1979**.
30. S.A. Umoren, E.E. Ebenso, The synergistic effect of polyacrylamide and iodide ions on the corrosion

inhibition of mild steel in H_2SO_4, Mater. Chem. Phys., **2007**, 106, 387-393.
31. T.A. Nyijime, F. Iorhuna, Theoretical study of 3-(4-hydroxyphenyl)-1-(4-nitrophenyl) prop-2-en-1-one and 3-(4-hydroxyphenyl)-1-phenylprop-2-en-1-one as corrosion inhibitors on mild steel, Applied Journal of Environmental Engineering Science, **2022**, 8(2), 2-8.
32. A.D. Becke, Density-functional thermochemistry. I. The effect of the exchange-only gradient correction, The Journal of Chemical Physics, **1992**, 96(3), 2155-2160.
33. T.A. Salman, K.A. Samawi, J.K. Shneine, Electrochemical and computational studies for mild steel corrosion inhibition by Benzaldehydethiosemicarbazone in acidic medium, Portugaliae Electrochimica Acta, **2019**, 37(4), 241-255.
34. C. Lee, W. Yang,R.G. Parr, Development of the Colle-Salvetti correlation-energy formula into a functional of the electron density, Physical Review B, **1988**, 37(2), 785.
35. T.A. Nyijime, H.F. Chahul, A.M. Ayuba, F. Iorhuna, Theoretical investigations on thiadiazole derivatives as corrosion inhibitors on mild steel, Advanced Journal of Chemistry-Section A, **2023**, 6, 141.
36. N.O. Obi-Egbedi, I.B. Obot, M.I. El-Khaiary, S.A. Umoren, E.E. Ebenso, Computational simulation and statistical analysis on the relationship between corrosion inhibition efficiency and molecular structure of some phenanthroline derivatives on mild steel surface, Int. J. Electrochem. Sci., **2011**, 6(1), 5649-5675.
37. C.B. Verma, M.A. Quraishi, A. Singh, 2-Aminobenzene-1, 3-dicarbonitriles as green corrosion inhibitor for mild steel in 1 M HCl: Electrochemical, thermodynamic, surface and quantum chemical investigation, Journal of the Taiwan Institute of Chemical Engineers, **2015**, 49, 229-239.
38. R. Kinkar Roy, K. Hirao, S. Krishnamurthy, S. Pal, Mulliken population analysis based evaluation of condensed Fukui function indices using fractional molecular charge, The Journal of Chemical Physics, **2001**, 15(7), 2901-2907.
39. H.H. Zhang, Y. Chen, Z. Zhang, Comparative studies of two benzaldehyde thiosemicarbazone derivatives as corrosion inhibitors for mild steel in 1.0 M HCl, Results in Physics, **2018**, 11, 554-563.
40. R. Pal, P.K. Chattaraj, Electrophilicity index revisited, Journal of Computational Chemistry, **2023**, 44(3), 278-297.
41. H. Zou, L.J. Arachchige, W. Rong, C. Tang, R. Wang, S. Tan, L. Duan, Low-Valence Metal Single Atoms on Graphdiyne Promotes Electrochemical Nitrogen Reduction via M-to-N2 π-Back donation, Advanced Functional Materials, **2022**, 32(24), 2200333.
42. E.S.M. Sherif, Effects of 2-amino-5-(ethylthio)-1,3,4-thiadiazole on copper corrosion as a corrosion inhibitor in 3% NaCl solutions, Appl. Surf. Sci., **2006**, 252, 8615-8623.
43. L. Guo, M. Zhu, J. Chang, R. Thomas, R. Zhang, P. Wang, R. Marzouki, Corrosion Inhibition of N80 Steel by Newly Synthesized Imidazoline Based Ionic Liquid in 15% HCl Medium: Experimental and Theoretical Investigations, International Journal of Electrochemical Science, **2021**, 16(11), 211139.
44. S.M. Shareef, Power quality enhancement by optimally placing the UPQC in the distribution system: A hybrid optimization model, Journal of Computational Mechanics, Power System and Control, **2021**, 4(1), 26-34.
45. M. Bouayed, H. Rabaa, A. Srhiri, J.Y. Saillard, A.B. Bachir, A. Le Beuze, Experimental and theoretical study of organic corrosion inhibitors on iron in acidic medium, Corrosion Science, **1999**, 41(3), 501-517.
46. G. Gece, S. Bilgiç, Quantum chemical study of some cyclic nitrogen compounds as corrosion inhibitors of steel in NaCl media, Corrosion Science, **2009**, 51(8), 1876-1878.
47. R.K. Roy, S. Pal, K. Hirao, On non-negativity of Fukui function indices, The Journal of chemical physics, **1999**, 110(17), 8236-8245.
48. R.R. Contreras, P. Fuentealba, M. Galván, P. Pérez, A direct evaluation of regional Fukui functions in molecules, Chemical Physics Letters, **1999**, 304(5-6), 405-413.
49. U. Umaru, A.M. Ayuba, Quantum chemical calculations and molecular dynamic simulation studies on the corrosion inhibition of aluminium metal by myricetin derivatives, Journal of New Technology and Materials, **2020**, 10(02), 18-28.